

## Non-perfect Synchronisation of $\beta$ -Scission with Product Stabilisation in Radical Ring-opening Reactions

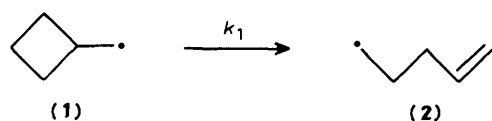
John C. Walton

University of St. Andrews, Department of Chemistry, St. Andrews, Fife KY16 9ST

Reduction of cyclobut-2-enylmethyl bromide with tri-*n*-butyltin hydride gave 3-methylcyclobutene together with *trans*- and *cis*-penta-1,3-diene and penta-1,4-diene. The diene products are formed by  $\beta$ -scission of the intermediate cyclobut-2-enylmethyl radicals to give pentadienyl radicals which accept hydrogen at the terminal and central carbon atoms. The rate constants and activation energies of  $\beta$ -scission in the series of radicals cyclobutylmethyl, 3-methylenecyclobutylmethyl, cyclobut-2-enylmethyl were shown to change little with the large increase in product radical stabilisation. This was accounted for in terms of the principle of non-perfect synchronisation, *i.e.* bond scission occurs before the development of resonance delocalisation. Semi-empirical MNDO calculations for the same series of radicals were in full agreement with this interpretation.

In carbanion-forming reactions the transition state is often imbalanced, *i.e.* bond cleavage and charge delocalisation have made unequal progress at the transition state. The evidence of this imbalance has recently been summarised and evaluated by Bernasconi<sup>1,2</sup> who proposed a 'principle of non-perfect synchronisation (PNS)'. According to this principle, a product-stabilising factor that develops late along the reaction co-ordinate lowers the intrinsic rate.<sup>2</sup> There have been a number of suggestions that the transition states of homolytic reactions are also imbalanced, and in particular that resonance stabilisation in the product of a radical addition reaction develops 'late' on the reaction co-ordinate.<sup>3,4</sup> It seemed possible that the PNS could help to rationalise kinetic data for several different types of radical reactions. Thus, it is well known that radicals such as  $H^\cdot$ ,  $CF_3^\cdot$ , and  $CH_3^\cdot$  add to buta-1,3-diene only about ten times as fast as to ethylene<sup>5,6</sup> even though the product radical of the former contains the large allyl stabilisation energy. This insensitivity of the rate constant to product stabilisation is certainly consistent with the PNS prediction. The rates of quite a number of intramolecular radical addition reactions, *i.e.* cyclisations, have been determined.<sup>7</sup> Substituents which hyperconjugatively stabilised the cyclised radical had little effect on the rate, as would be expected from the PNS. However, even in the most studied case, that of hex-5-enyl, kinetic data were not available for a sufficiently wide range of radicals for firm conclusions to be drawn.

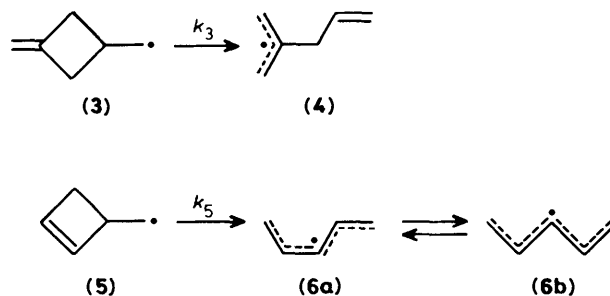
The reverse of the cyclisation reaction is ring opening by  $\beta$ -scission. This process is rapid for cyclopropylmethyl and cyclobutylmethyl radicals (1) where the relief of ring strain leads to exothermic rearrangement. The rates of ring opening of a number of radicals of type (1) have been determined.<sup>8-10</sup> The



activation energies for  $\beta$ -scission of a very restricted range of these radicals correlate with the rearrangement enthalpies<sup>10</sup> but exceptions and anomalies were noted.<sup>8,10</sup> In this paper we show that the 3-methylenecyclobutylmethyl radical (3) and cyclobut-2-enylmethyl radical (5) rearrangements provide extreme examples of imbalanced transition states.

### Results and Discussion

*Kinetics of Ring Opening for Cyclobutylmethyl-type Radicals.*—The ring opening of cyclobutylmethyl (1), 3-methylenecyclobutylmethyl (3), and cyclobut-2-enylmethyl radicals (5) provides a series of homolytic rearrangements in which the stabilisation energy of the product radical successively increases



from zero in (2) to allyl stabilisation in (4) and to pentadienyl stabilisation in (6). If bond scission was synchronised with the development of resonance stabilisation in the product, a very large increase in rate, and reduction in the activation energy, would be expected along this series.

The rate of ring opening of (1) was determined by reduction of the corresponding chloride with tri-*n*-butyltin hydride by Beckwith and Moad.<sup>8</sup> This gave the rate of rearrangement relative to the rate of hydrogen abstraction from  $Bu_3SnH$  ( $k_H$ ) by the primary radicals (2). The absolute rate constants  $k_1$  can be obtained by using the  $k_H$  values determined by laser flash photolysis experiments of Ingold and his co-workers.<sup>11</sup> The  $k_1$  values were also obtained in a different temperature range, relative to the termination rate constant  $2k_t$  of the radical (2), by kinetic e.s.r. experiments.<sup>9</sup> The absolute  $k_1$  values were then obtained by use of the accurate  $2k_t$  values for *t*-butyl radicals determined by Fischer and his co-workers,<sup>12</sup> corrected for the differences in viscosity of the solvents. When plotted in Arrhenius form the two sets of data form a single straight line (Figure 1).

The rate constants  $k_3$  for  $\beta$ -scission of radical (3) were determined recently both by  $Bu_3SnH$  reduction of the corresponding bromide and by kinetic e.s.r. experiments.<sup>13</sup> The data are shown as an Arrhenius plot in Figure 1.

The ring opening of radical (5) was studied by using the

**Table 1.** Products<sup>a</sup> of the reduction of cyclobut-2-enylmethyl bromide with tri-*n*-butyltin hydride<sup>b</sup>

| <i>T</i> /°C | 10 <sup>3</sup> [(8)] | 10 <sup>3</sup> [(9)] | 10 <sup>3</sup> [(10)] | 10 <sup>3</sup> [(11)] |
|--------------|-----------------------|-----------------------|------------------------|------------------------|
| 21           | 53.0                  | 0.91                  | 0.04                   |                        |
| 51           | 34.6                  | 2.57                  | 0.39                   |                        |
| 77           | 45.6                  | 8.41                  | 1.48                   | 0.15                   |
| 96           | 75.7                  | 27.1                  | 5.32                   | 0.56                   |
| 139          |                       | 52.1                  | 13.7                   | 3.25                   |

<sup>a</sup>In mol dm<sup>-3</sup>. <sup>b</sup>[Bu<sub>3</sub>SnH] 0.776 mol dm<sup>-3</sup>, [(7)] 0.155 mol dm<sup>-3</sup>. Reactions in *t*-butylbenzene (0.5 cm<sup>3</sup>).

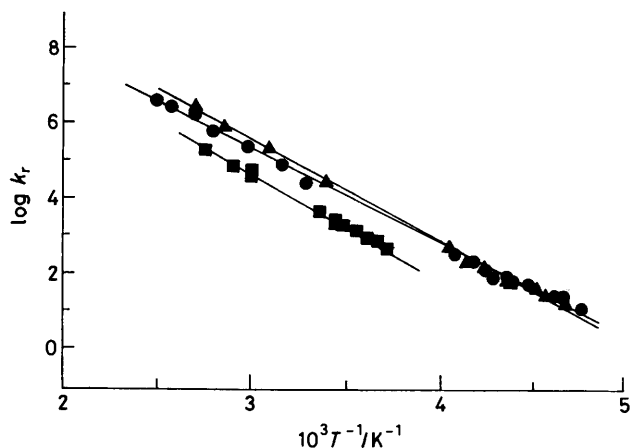
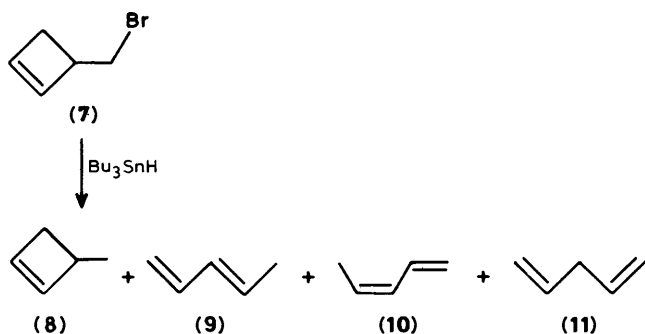


**Figure 1.** Arrhenius plots of rearrangement rate constants for cyclobutylmethyl-type radicals. Squares: radicals (1), high-temperature group of points are tin hydride results of Beckwith and Moad;<sup>8</sup> low-temperature group are kinetic e.s.r. results.<sup>9</sup> Circles: radical (3), high-temperature group of points, tin hydride results; low-temperature group, kinetic e.s.r. data.<sup>13</sup> Triangles: radical (5), high-temperature group of points, tin hydride results; low-temperature group, kinetic e.s.r. data

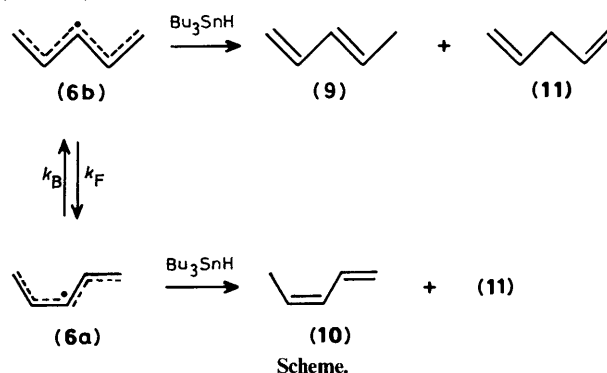
reduction of cyclobut-2-enylmethyl bromide (7) with tri-*n*-butyltin hydride. Four products, 3-methylcyclobutene (8), *trans*-penta-1,3-diene (9) and *cis*-penta-1,3-diene (10), and penta-1,4-diene (11) were detected. The amounts of these products formed at each temperature are given in Table 1.

Product (11) is formed when hydrogen is transferred to the central C(3) of the intermediate pentadienyl radical (6a or b). The spin density at C(3) in (6a and b) is slightly greater than at the radical termini C(1) and C(5)<sup>14</sup> and this suggests that significant amounts of (11) should be formed. However, (11) is disfavoured because it lacks the conjugation stabilisation which is present in the products (9) and (10) formed when radical (6) abstracts at either terminus. Product (11) is also disfavoured by



a statistical factor of two and by a steric effect; C(3) is shielded by two substituents in comparison with only one at C(1) or C(5). The small amount of (11) is not therefore surprising and in fact the products derived from attack at the central, bisallylic site in dienes are not usually detectable. For example, in the autoxidation of bisallylic dienes like linoleic acid, no products derived from the central site in the intermediate radical have been observed.<sup>15,16</sup> It has been suggested that oxygen entrapment at the central carbon atom of the pentadienyl system does occur in polyunsaturated lipid autoxidation but that the peroxy radicals rearrange to give the thermodynamically more stable conjugated dienehydroperoxides.<sup>17</sup> The isolation of significant amounts of (11) in the present work supports this conclusion.

The ratio of *cis*- (10) to *trans*- (9) dienes varies from 0.04 at 21 °C to 0.26 at 139 °C. These ratios are somewhat higher than the equilibrium ratio of the radical concentrations [(6a)]:[(6b)] as calculated from the known *k<sub>F</sub>* and *k<sub>B</sub>* values at each temperature.<sup>18</sup> However, the error limits on *k<sub>F</sub>* and *k<sub>B</sub>* are quite large and we can conclude that the [(10)]:[(9)] product ratio probably reflects the equilibrium radical ratio. Thus, to within the experimental error, the *trans* radical (6b) gives exclusively the *trans* product and the *cis* radical (6a) gives the *cis* product (10) but both radicals can give the bisallylic product (11) (Scheme).



The rate constant ratio *k<sub>5</sub>*:*k<sub>H</sub>*, where *k<sub>H</sub>* is the rate constant for hydrogen abstraction by radicals (5) and (6) from Bu<sub>3</sub>SnH, was evaluated from the total rearranged and unrearranged product using an integrated rate equation<sup>8,18</sup> (Figure 1). The ring opening of (5) was examined previously by kinetic e.s.r. spectroscopy.<sup>9</sup> The *k<sub>5</sub>* values obtained from that study by using Fischer's<sup>12</sup> parameters for 2*k<sub>i</sub>* are also plotted in Figure 1.

Examination of Figure 1 shows that excellent Arrhenius lines were obtained for all three rearrangements. This demonstrates that the tin hydride method and the kinetic e.s.r. method are consistent with one another and give reliable rate data, *i.e.* the *k<sub>H</sub>* and 2*k<sub>i</sub>* 'master clocks' tell the same time. The rearrangements of (1), (3), and (5) have each been examined by two independent kinetic methods and their rates of unimolecular ring opening are therefore amongst the best established 'free radical clocks'. The Arrhenius parameters are given in Table 2. The remarkable result which Table 2 reveals is the small change in the rate constant with increasing exothermicity of the rearrangement. In fact, the activation energies for all three rearrangements are of similar magnitude and most of the increase in the rate constants is the result of the increasing exponential factors.

Comparison of the kinetic parameters for radicals (3) and (5) with those of cyclopropylmethyl<sup>19</sup> (Table 2) shows just how insensitive the rearrangement rate constants of the former radicals are to increased exothermicity of the reaction. For cyclopropylmethyl a modest increase in exothermicity due to the greater ring strain leads to a rate increase of more than four

**Table 2.** Arrhenius parameters for ring opening of cyclobutylmethyl and related radicals

| Radical                          | $k/s^{-1}$ (25 °C) | $E/kcal\ mol^{-1}$ | $\log(A/s^{-1})$ |
|----------------------------------|--------------------|--------------------|------------------|
| Cyclobutylmethyl (1)             | $4.7 \times 10^3$  | 12.2               | 12.6             |
| 3-Methylene-cyclobutylmethyl (3) | $28.0 \times 10^3$ | 11.5               | 12.9             |
| Cyclobut-2-enylmethyl (5)        | $39.2 \times 10^3$ | 12.5               | 13.8             |
| Cyclopropylmethyl <sup>a</sup>   | $1.3 \times 10^8$  | 5.9                | 12.5             |

<sup>a</sup> Data from ref. 19.**Table 3.** Thermochemistry of cyclobutylmethyl and related rearrangements

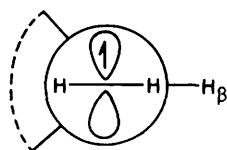
| $\beta$ -Scission of | RS <sup>a</sup> | $\Delta H^{\circ b}$ |
|----------------------|-----------------|----------------------|
| (1)                  | 26.2            | -4.4                 |
| (3)                  | 28.5            | -19.6 <sup>c</sup>   |
| (5)                  | 29.8            | -28.1 <sup>d</sup>   |
| Cyclopropylmethyl    | 27.6            | -5.9                 |

<sup>a</sup> Conventional ring strain in kcal mol<sup>-1</sup>. <sup>b</sup> Calculated from Benson's Group Contributions.<sup>25</sup> <sup>c</sup> Assuming SE(allyl) 12.6 kcal mol<sup>-1</sup>. <sup>d</sup> Assuming SE(pentadienyl) 18.5 kcal mol<sup>-1</sup>.

orders of magnitude. Of course, other factors may also contribute to this increase.

The  $\beta$ -hydrogen hyperfine splittings (h.f.s.) of radicals (1), (3), and (5) are 1.4, 1.4, and 1.1 mT respectively at 220 K and all show a smooth increase with increasing temperature. Thus these radicals all adopt the same preferred conformation (12), as does cyclopropylmethyl, in which the SOMO can readily eclipse the breaking C <sub>$\beta$</sub> -C <sub>$\gamma$</sub>  bond. Thus all the rearrangements are stereoelectronically allowed, *i.e.* this stereoelectronic factor does not provide any rationale of the observed kinetic data.

The allyl stabilisation energy (SE) has been variously estimated<sup>20-22</sup> in the range 11.5 to 14.5 kcal mol<sup>-1</sup>\* and measurements of SE(pentadienyl) range from 18.5 to 24.5 kcal mol<sup>-1</sup>.<sup>20,23,24</sup> The enthalpies of the rearrangements, estimated by the Group Contributions method,<sup>25</sup> are in Table 3. In deriving the enthalpies of formation of radicals (4) and (6) the allyl and pentadienyl SEs have been taken as 12.6 and 18.5 kcal mol<sup>-1</sup>, respectively, because these are the values derived from thermochemical experiments and they are consistent with the other thermochemical data embodied in the Group Contributions. These estimates show a small increase in ring strain across the series (1), (3), and (5) and the expected very large increase in rearrangement exothermicity. Thus, neither the stereoelectronic factor, nor the thermochemistry, can rationalise the kinetic data of the rearrangements. It appears therefore that the resonance stabilisation of radicals (4) and (6) develops late on the reaction co-ordinate and is not 'felt' by the transition state.



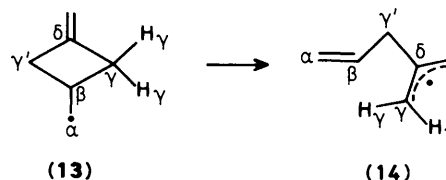
(12)

Thus the  $\beta$ -scission is not synchronised with the development of resonance stabilisation and the transition state is imbalanced. According to the PNS (see above) late development of product stabilisation leads to a decrease in intrinsic rate. In the case of radicals (3) and (5) the potentially very high rates of  $\beta$ -scission are not therefore achieved and the decrease in rate due to non-synchronisation brings the activation energy of rearrangement down to about the same value as for radical (1). Ring opening for the series (1), (3), (5) seems to provide an apt illustration of the working of the PNS.

It is not difficult to understand why the product stabilisation develops late, in terms of the molecular geometry. In radical (3) scission of the C <sub>$\beta$</sub> -C <sub>$\gamma$</sub>  bond must be followed by flattening at C <sub>$\gamma$</sub>  and rotation through 90° before maximum resonance stabilisation can develop. In radical (5)  $\beta$ -scission must be followed by flattening and rotation at both C <sub>$\beta$</sub>  and C <sub>$\gamma$</sub> . That these geometrical changes occur after significant lengthening of the C <sub>$\beta$</sub> -C <sub>$\gamma$</sub>  bond is not so surprising. What is surprising, however, is the almost total decoupling of these effects. In spite of the large potential lowering of energy available from resonance stabilisation, the molecules prefer to rearrange in a completely non-synchronous mode.

*Semi-empirical SCF MO Calculations.*—The  $\beta$ -scission of radicals (1) and (5) was previously investigated using the MINDO/3 method.<sup>26</sup> In the present work  $\beta$ -scission of radicals (1), (3), and (5) was followed using the MNDO approach.<sup>27</sup> For each radical the appropriate C <sub>$\beta$</sub> -C <sub>$\gamma$</sub>  bond was chosen as the reaction co-ordinate and the enthalpy of formation was computed for successive increments thereof. All other geometrical parameters were optimised for each value of the C <sub>$\beta$</sub> -C <sub>$\gamma$</sub>  bond length. Best results were obtained by starting with the geometry of the ring-opened radical and successively reducing the C <sub>$\beta$</sub> -C <sub>$\gamma$</sub>  bond length. In the case of radical (3) a small 'jump' (*ca.* 1 kcal mol<sup>-1</sup>) was found between 2.36 and 2.37 Å and for (5) a 'jump' (*ca.* 5 kcal mol<sup>-1</sup>) between 2.24 and 2.25 Å. This was quite reproducible but was ignored because it occurs well after the transition state.

The computations show a very consistent pattern of behaviour (Table 4). For all three radicals the C <sub>$\beta$</sub> -C <sub>$\gamma$</sub>  bond extends from an initial value of *ca.* 1.57 to *ca.* 2.05 Å in the transition state. At the same time the C <sub>$\alpha$</sub> -C <sub>$\beta$</sub>  bond which initially is somewhat shorter than a normal C-C bond [C <sub>$\alpha$</sub> -C <sub>$\beta$</sub>  *ca.* 1.48 Å in (1), (3), and (5)] reduces to *ca.* 1.36 Å, *i.e.* becomes almost a fully formed double bond. The development of resonance stabilisation is best monitored by means of the dihedral angle H <sub>$\gamma$</sub> -C <sub>$\gamma$</sub> -C <sub>$\delta$</sub> -C <sub>$\gamma'$</sub>  ( $\equiv \phi$ ). This starts at *ca.* 116° in the four-



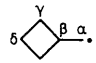
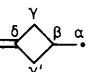
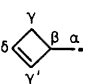
(13)

(14)

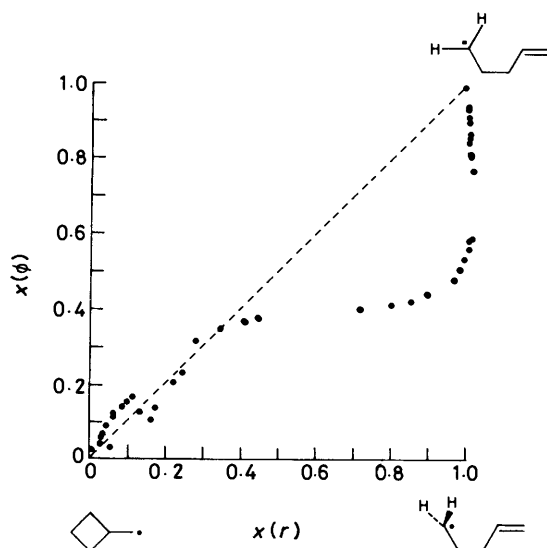
membered ring of each radical, *e.g.* (13) and reduces to 0° for full development of resonance stabilisation in the product radical, *e.g.* (14). The computations showed (Table 4) that for all three radicals  $\phi$  had reduced by only 10° to *ca.* 106° in the transition state, *i.e.* there was no significant development of resonance delocalisation. The MNDO calculations overestimated the enthalpies of reaction ( $\Delta H^{\circ}$ ) and enthalpies of activation ( $\Delta H^{\ddagger}$ ) (*cf.* Tables 2 and 3) but did produce the right trends, *i.e.*  $\Delta H^{\circ}$  decreasing along the series (1), (3), (5) and relatively minor changes in  $\Delta H^{\ddagger}$  along the same series.

\* 1 cal  $\equiv$  4.18 J.

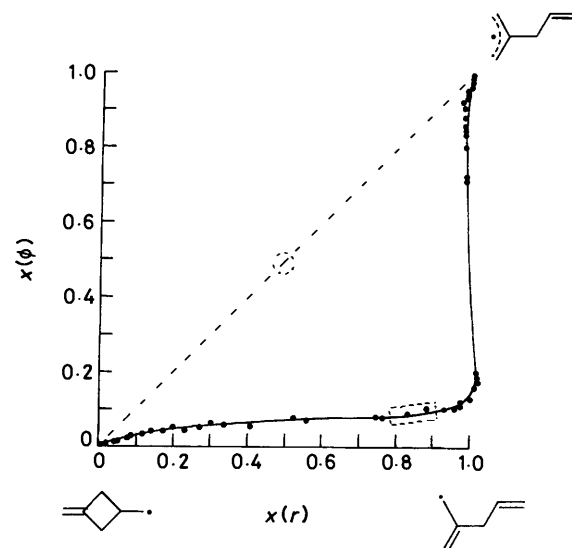
**Table 4.** MNDO Calculations for cyclobutylmethyl-type radicals

| Radical                                                                           | $\Delta H^{\ddagger a}$ | $\Delta H^{\ddagger b}$ | $C_{\beta}-C_{\gamma}^{\ddagger c}$ | $C_{\alpha}-C_{\beta}^{\ddagger d}$ | $\phi^e$ |
|-----------------------------------------------------------------------------------|-------------------------|-------------------------|-------------------------------------|-------------------------------------|----------|
|  | 12.1                    | 37.4                    | 2.054                               | 1.361                               | 106      |
|  | 11.1                    | 36.6                    | 2.056                               | 1.364                               | 106      |
|  | -9.7                    | 29.9                    | 2.038                               | 1.371                               | 103      |

<sup>a</sup> Computed enthalpy of  $\beta$ -scission in kcal mol<sup>-1</sup>. <sup>b</sup> Computed enthalpy of activation in kcal mol<sup>-1</sup>. <sup>c</sup> Bond lengths (Å) in the transition state. <sup>d</sup>  $C_{\alpha}-C_{\beta}$  bond length (Å) in the transition state. <sup>e</sup> Dihedral angle (°)  $H_{\gamma}-C_{\gamma}-C_{\delta}-C_{\alpha}$  (see text).

**Figure 2.** More O'Ferrall-Jencks diagram for radical (1)  $\beta$ -scission. Dots: progress variables computed by the MNDO method. Dashed line: ideal trajectory for perfect synchronisation

The computed results are plotted in the form of O'Ferrall-Jencks (MOF-J) diagrams<sup>28,29</sup> for radicals (1) and (3) in Figures 2 and 3, respectively. The lower left corner represents the unrearranged cyclobutylmethyl radical and the upper right corner represents the product radical. The lower right corner represents a hypothetical intermediate in which scission of the  $C_{\beta}-C_{\gamma}$  bond is complete but no resonance stabilisation has developed, *i.e.* the unpaired electron is localised on  $C_{\gamma}$ . The degree of  $\beta$ -scission [ $x(r)$ ] was plotted along the  $x$ -axis and the degree of electron delocalisation was plotted along the  $y$ -axis. The best measure of  $x(r)$  was found to be the  $C_{\alpha}-C_{\beta}$  bond length which changes from single to double during  $\beta$ -scission. The  $C_{\beta}-C_{\gamma}$  bond length itself was less satisfactory because this bond lengthens significantly in the final stages of the rearrangement

**Figure 3.** More O'Ferrall-Jencks diagram for radical (3)  $\beta$ -scission. Dots show the progress variables computed by the MNDO method; the transition state is boxed. Dotted line is the ideal trajectory for perfect synchronisation

owing to conformational changes in the product radical. The development of resonance delocalisation was satisfactorily represented by the changes in  $\phi$ , as described above, *i.e.* the degree of change in the dihedral angle  $x(\phi)$  was used to monitor the degree of stabilisation.

If  $\beta$ -scission were synchronised with the development of resonance stabilisation, the MOF-J plot would be a straight line at 45° joining the lower left and upper right corners (dashed line in Figures 2 and 3). For radical (1) there is no resonance delocalisation in the product and hence this rearrangement is expected to approximately follow the diagonal line.

Figure 2 shows that the MOF-J plot for (1) does follow the ideal diagonal line in the first half of the rearrangement but that a 'bulge' below the diagonal develops in the second half of the reaction. This 'bulge' develops because bond scission occurs more rapidly than dihedral rotation in the later stages of the reaction. In the product radical (2) there is no resonance stabilisation to 'control' the dihedral angle  $\phi$  which consequently responds mainly to conformational changes. Thus, the 'bulge' in this case does not invalidate the method but shows that  $\phi$  is not the ideal choice of progress variable in the absence of product stabilisation.

The MOF-J plot for radical (3) follows a strongly curved path below the diagonal, exactly as would be expected for a non-synchronous rearrangement. In practice, the computations show a small 'overshoot' in the  $x(r)$  variable which increases slightly beyond 1.0 before returning to 1.0 after rotation brings about resonance stabilisation. This could be a real effect, but it might also be due to non-ideal behaviour of the optimisation algorithm in the MNDO program. The MOF-J plot of the MNDO results for radical (5) was very similar indeed to Figure 3. These MOF-J plots curve almost as far below the diagonal as is theoretically possible, which indicates that the rearrangements are rather extreme cases of non-synchronous reactions. For both (3) and (5) the  $\beta$ -scission is predicted to be *ca.* 85% complete in the transition state, but only *ca.* 10% resonance stabilisation has developed. The semi-empirical calculations agree very well with the conclusions drawn from the kinetic results. The kinetics of radical ring-opening reactions and radical addition reactions, where the product contains resonance stabilisation, can be understood in terms of the

principle of non-perfect synchronisation, *i.e.* this principle applies to homolytic reactions as well as carbanion-forming reactions.

### Experimental

N.m.r. spectra were recorded with a Bruker WP 80 instrument on  $\text{CDCl}_3$  solutions at ambient temperature with tetramethylsilane as internal standard. G.c.-m.s. analysis was carried out with a Finnegan Incos instrument. G.l.c. analyses were made on a Pye-Unicam PU 4500 chromatograph using 2 m columns packed with 20% BMEA on Chromosorb P, 80–100 mesh or 10% Carbowax 20 M.

*Reduction of Cyclobut-2-enylmethyl Bromide (7) with  $\text{Bu}_3\text{SnH}$ .*—Bromide (7) (20  $\mu\text{l}$ ) available from previous work<sup>14</sup> and  $\text{Bu}_3\text{SnH}$  (240  $\mu\text{l}$ ) in *t*-butylbenzene (0.5 ml) were degassed by bubbling nitrogen for 15 min and then photolysed in a thin-wall Pyrex tube for 1 h at 50 °C. Several such reactions were combined and the volatile components were distilled out on a vacuum line. G.l.c. analysis showed one major product together with *t*-butylbenzene and traces of three other products. The  $^1\text{H}$  n.m.r. spectrum of the mixture showed *t*-butylbenzene together with 3-methylcyclobutene (8); the spectrum of the latter was identical to that given in the literature.<sup>14</sup> The mixture was also examined by coupled g.c.-m.s. The major product had  $M^+$  68 and a fragmentation pattern consistent with structure (8). Of the three minor products, the most important had  $M^+$  68 and a fragmentation pattern identical with that of *trans*-penta-1,3-diene (9). The mass spectra from the remaining two products were too weak for identification but retention time comparisons with authentic materials on two columns showed these to be penta-1,4-diene (11) and *cis*-penta-1,3-diene (10). The *trans*-penta-1,3-diene was also confirmed by retention time comparisons. The g.c.-m.s. also showed the presence of minor amounts of unchanged bromide.

*Kinetics of the Reduction of (7) with  $\text{Bu}_3\text{SnH}$ .*—*t*-Butylbenzene (0.50 ml) was placed in a Pyrex tube, heated to the desired temperature, and degassed by bubbling nitrogen for *ca.* 15 min. To this was added the bromide (10  $\mu\text{l}$ , 0.16 mol  $\text{l}^{-1}$ ),  $\text{Bu}_3\text{SnH}$  (120  $\mu\text{l}$ , 0.776 mol  $\text{l}^{-1}$ ), and cyclohexane (5  $\mu\text{l}$ , 0.073 mol  $\text{l}^{-1}$ ) as internal standard. The solution was photolysed for 60 min with light from a 250 W medium-pressure mercury arc and then analysed with the BMEA column. The  $k_5/k_H$  values were obtained at each temperature from the final product concentrations and the initial  $\text{Bu}_3\text{SnH}$  concentration using an integrated rate equation. The best values of  $k_5/k_H$  were located

with an iterative computer program based on NAG routine COSAXF.

### References

- 1 C. F. Bernasconi, *Tetrahedron*, 1985, **41**, 3219.
- 2 C. F. Bernasconi, *Acc. Chem. Res.*, 1987, **20**, 301.
- 3 J. M. Tedder and J. C. Walton, *Adv. Phys. Org. Chem.*, 1978, **16**, 51.
- 4 J. M. Tedder and J. C. Walton, *Tetrahedron*, 1980, **36**, 701.
- 5 R. J. Cvetanović and R. S. Irwin, *J. Chem. Phys.*, 1967, **46**, 1694.
- 6 J. A. Kerr in 'Free Radicals,' ed. J. K. Kochi, Wiley-Interscience, New York, 1973, vol. 1, ch. 1, p. 1.
- 7 A. L. J. Beckwith and K. U. Ingold in 'Rearrangements in Ground and Excited States,' ed. P. de Mayo, Academic Press, New York, 1980, vol. 1, p. 161.
- 8 A. L. J. Beckwith and G. Moad, *J. Chem. Soc., Perkin Trans. 2*, 1980, 1083.
- 9 K. U. Ingold, B. Maillard, and J. C. Walton, *J. Chem. Soc., Perkin Trans. 2*, 1981, 970.
- 10 B. Maillard and J. C. Walton, *J. Chem. Soc., Perkin Trans. 2*, 1985, 443.
- 11 C. Chatgililoglu, K. U. Ingold, and J. C. Scaiano, *J. Am. Chem. Soc.*, 1981, **103**, 7739.
- 12 H. Schuh and H. Fischer, *Int. J. Chem. Kinet.*, 1976, **8**, 341.
- 13 J. C. Walton, *J. Chem. Soc., Perkin Trans. 2*, 1987, 231.
- 14 A. G. Davies, D. Griller, K. U. Ingold, D. A. Lindsay, and J. C. Walton, *J. Chem. Soc., Perkin Trans. 2*, 1981, 633.
- 15 J. F. Mead in 'Free Radicals in Biology,' ed. W. A. Pryor, Academic Press, New York, 1976, vol. 1, p. 51.
- 16 N. A. Porter, B. A. Weber, H. Weenen, and J. A. Khan, *J. Am. Chem. Soc.*, 1980, **102**, 5597.
- 17 E. Bascetta, F. D. Gunstone, and J. C. Walton, *J. Chem. Soc., Perkin Trans. 2*, 1983, 603.
- 18 A. L. J. Beckwith and G. Moad, *J. Chem. Soc., Chem. Commun.*, 1974, 472.
- 19 B. Maillard, D. Forest, and K. U. Ingold, *J. Am. Chem. Soc.*, 1976, **98**, 7024.
- 20 J. C. Walton, *Rev. Chem. Intermed.*, 1984, **5**, 249.
- 21 A. B. Trenwith, *J. Chem. Soc., Faraday Trans. 1*, 1973, **69**, 1737.
- 22 M. Rossi, K. D. King, and D. M. Golden, *J. Am. Chem. Soc.*, 1979, **101**, 1223; M. Rossi and D. M. Golden, *ibid.*, p. 1230.
- 23 A. B. Trenwith, *J. Chem. Soc., Faraday Trans. 1*, 1980, **76**, 266; 1982, **78**, 3131.
- 24 D. F. McMillen and D. M. Golden, *Annu. Rev. Phys. Chem.*, 1982, **33**, 493.
- 25 S. W. Benson, 'Thermochemical Kinetics,' Wiley, New York, 1976, 2nd edn., pp. 73, 272, 273.
- 26 J. R. Bews, C. Glidewell, and J. C. Walton, *J. Chem. Soc., Perkin Trans. 2*, 1982, 1447.
- 27 J. J. P. Stewart, Quantum Chemistry Program Exchange, University of Indiana, Indiana, 1983, No. 455.
- 28 R. A. More O'Ferrall, *J. Chem. Soc. B*, 1970, 274.
- 29 D. A. Jencks and W. P. Jencks, *J. Am. Chem. Soc.*, 1977, **99**, 7948.

Received 28th April 1988; Paper 8/01669